

Waypoint Tracking via Tube-based Robust Model Predictive Control for Crop Monitoring with Fixed-Wing UAVs

*Original*

Waypoint Tracking via Tube-based Robust Model Predictive Control for Crop Monitoring with Fixed-Wing UAVs / Mammarella, M., Ristorto, G., Capello, E., Bloise, N., Guglieri, G., Dabbene, F.. - ELETTRONICO. - (2019), pp. 19-24. (2019 IEEE International Workshop on Metrology for Agriculture and Forestry Portici (ITA) 24-26/10/2019) [10.1109/MetroAgriFor.2019.8909260].

*Availability:*

This version is available at: 11583/2764432 since: 2019-10-30T14:25:53Z

*Publisher:*

IEEE

*Published*

DOI:10.1109/MetroAgriFor.2019.8909260

*Terms of use:*

This article is made available under terms and conditions as specified in the corresponding bibliographic description in the repository

*Publisher copyright*

IEEE postprint/Author's Accepted Manuscript

©2019 IEEE. Personal use of this material is permitted. Permission from IEEE must be obtained for all other uses, in any current or future media, including reprinting/republishing this material for advertising or promotional purposes, creating new collecting works, for resale or lists, or reuse of any copyrighted component of this work in other works.

(Article begins on next page)

# Waypoint Tracking via Tube-based Robust Model Predictive Control for Crop Monitoring with Fixed-Wing UAVs

Martina Mammarella<sup>1,2</sup>, Gianluca Ristorto<sup>3</sup>, Elisa Capello<sup>1,4,5</sup>, Nicoletta Bloise<sup>4</sup>,  
Giorgio Guglieri<sup>\*,1,4,5</sup>, and Fabrizio Dabbene<sup>1</sup>

<sup>1</sup> *Institute of Electronics, Computer and Telecommunication Engineering, National Research Council of Italy, Turin, Italy*  
martina.mammarella@ieiit.cnr.it, fabrizio.dabbene@ieiit.cnr.it

<sup>2</sup> *Dipartimento di Scienze Agrarie, Forestali e Alimentari, Università degli Studi di Torino, Turin, Italy*

<sup>3</sup> *MAVTECH s.r.l. c/o NOI Techpark Südtirol/Alto Adige, Via Ipazia 2, 39100 Bozen, Italy*  
gianluca.ristorto@mavtech.eu

<sup>4</sup> *Department of Mechanical and Aerospace Engineering, Politecnico di Torino, Turin, Italy*  
elisa.capello@polito.it, nicoletta.bloise@polito.it, giorgio.guglieri@polito.it

<sup>5</sup> *PICASeR - Politecnico Interdepartmental Centre for Service Robotics, Politecnico di Torino, Turin, Italy*

**Abstract**—Crop monitoring and farm activities with innovative systems, as Unmanned Aerial Vehicles, is an undergoing research known as *fourth agricultural revolution*. In our paper, two different farming scenarios are proposed, in which a trajectory tracking based on Model Predictive Control is proposed in combination with a waypoint-based guidance algorithm. This Guidance and Control algorithm is also combined with an on-board sensor to characterize the measured data. Simulations are performed to show the effectiveness of the proposed control scheme.

**Index Terms**—Crop Monitoring, Precision Farming, Unmanned Aerial Vehicle, Robust Model Predictive Control

## I. INTRODUCTION

Farming is finally undergoing the so-called fourth agricultural revolution, thanks to the introduction of emerging technologies as robotics and artificial intelligence, aiming at improving the output and sustainability of plantations, quality of products and working conditions [1]. The Food and Agriculture Organization of the United Nations (FAO) and the International Telecommunication Union (ITU) have been collaborating together with partners to address some of the challenges faced in agriculture through the use of sustainable Information and Communication Technologies (ICTs). One of the latest development is represented by the increased use of small, Unmanned Aerial Vehicles (UAVs) for agriculture. These systems, also known as drones, have a great potential to support and address some of the most pressing challenges in farming. As clearly explained in the second series of *E-Agriculture in Action* published by FAO [2], real-time quality data and crop monitoring are two of these challenges. Indeed, UAVs could represent a favorable alternative to conventional farming machines, whenever clear advantages with respect to traditional methods, in terms of higher efficiency in operations,

reduced environmental impact or enhanced human health and safety are sought.

One of the most challenging agriculture remote sensing scenarios, which would mostly benefit from the support provided by UAVs, is represented by vineyards. These fields are characterized by vast areas, scarce maneuver space, and steep and sloped soils. Lately, a relevant number of research projects focused on the exploitation of drones for site-specific vineyard management [3] and monitoring [4], vineyard variability assessment [5], and grapevine disease detection [6]. Among them, it is possible to observe a large use of *multi-rotor* UAVs, characterized by a high degree of maneuverability and flexibility in configuration. However, their high fuel consumption, limited flight autonomy, and relative low speed have recently stirred the interest in employing fixed-wing UAVs (FW-UAVs). As highlighted in [7], these FW-UAVs are in general able to perform longer missions and to cover larger areas, and have lower development and maintenance costs. Envisioning remote sensing applications, UAVs are able to provide trajectory tracking capability and stability performance thanks to tailored advanced control schemes. Combining the need of tackling mission, system and mechanical constraints with the need of guaranteeing robustness to external, bounded disturbances, which could compromise the controller performance, several robust MPC techniques have been proposed for remote sensing applications as in [8] and [9].

The main objective of this paper is to propose a low-cost and high-throughput method for a crop monitoring system, which uses a fixed-wing UAV as an operating platform. The key feature of the proposed approach is the design of ad-hoc guidance and control algorithms able to perform the desired mapping, guaranteeing robustness of the system to external disturbances, optimizing the path, for crop monitoring. Moreover, the use of a fixed-wing UAV is justified by the need to cover a huge terrain extension and, in combination with the

This work was funded by the Italian Institute of Technology (IIT) and the Italian Ministero dell'Istruzione, dell'Università e della Ricerca within the 2017 Projects of National Interest (PRIN 2017 N. 2017S559BB).

payload (i.e. sensor), the information can be post-processed or processed in real time to obtain an operative map. Thus, the UAV can incorporate in its system the designed map and optimally distribute, through capsule dropping techniques, seeds, fertilizer and so on.

In this paper, a robust MPC approach is proposed, which allows to reduce the *online* computational effort by pre-computing *offline* the feedback gain matrix  $K$  and the tightened constraints sets, to guarantee closed-loop system stability and robust constraint satisfaction, respectively, in the presence of bounded, additive disturbance. The so-called Tube-based Robust MPC (TRMPC) [10] is based on the concept of *tube* of trajectories. The main idea is to control the related undisturbed trajectory subject to tightened constraints in order to guarantee, for every possible disturbance realization within a predefined convex set, that the correspondent uncertain trajectory will lie within the desired constraint boundaries, as described in [10]. This approach has been already applied and in some cases experimentally validated in different fields such as automotive [11] and satellite [12]. Tracking TRMPC has been also proposed for robust tracking control of Planar Vertical Take-Off and Landing (PVTOL) aircraft in [13]. In this work, two tracking TRMPC schemes have been implemented for controlling both the longitudinal and lateral-directional error dynamics of a mini FW-UAV, for trajectory and terrain tracking missions. In particular, two different scenarios have been considered in which a FW-UAV is called to accomplish remote sensing tasks: (i) a flat paddy field; and (ii) a vineyard area.

The proposed approach combines the waypoint-based guidance strategy proposed in [14] with a tracking-based TRMPC scheme [10] to guarantee robust tracking constraint fulfillment and to improve FW-UAV performance with respect to classical approaches. To properly evaluate the reliability of the proposed guidance and control scheme, the classical multi-step software verification&validation approach for model-based design has been followed. As described in [15], the first step, which represent the main goal of this work, consists in performing Software-In-the-Loop (SIL) testing, i.e. executing the controller algorithm for non-real-time execution on the same host platform that is used by the modeling environment.

The remainder of the paper is organized as follows. The MH850 FW-UAV and the selected remote sensing scenarios are presented in Section II. Section III provides an overview of the simulation environment exploited for SIL testing, together with the waypoint-based guidance algorithm (Section III-A) and the tracking TRMPC scheme (III-B). Preliminary SIL results related to the paddy field an vineyard scenarios are provided in Section IV. Finally, conclusions and future works are drawn in Section V.

## II. THE MH850 AND SELECTED MONITORING SCENARIOS

### A. UAV Description

The MicroHawk aerial vehicles have been developed in order to perform reconnaissance and territorial monitoring, allowing a full interaction with ground control through a

real-time up and down data-link with the aircraft. The Mi-



Fig. 1: The MicroHawk MH850 FW-UAV (credit:MAVTech).

croHawk MH850 is a fixed wing, tailless integrated wing-body configuration UAV, which guarantees wider mission range and longer endurance, with respect to other existing concepts. Moreover, being a scaled UAV platform with a wingspan of 850 mm and a weight of about 1000 g, it provides flexibility with reduced cost and risk. A flight control system, providing automatic stability, guidance, navigation and control capabilities, is installed on the vehicle autopilot and allows to evaluate flight parameters either in real-time or in post-flight mode. The MH850 is able to carry a payload up to 100 g, excluding batteries, its airspeed ranges from 7.5 m/s up to 20 m/s, and has an endurance of about 75 min @ 12.5 m/s.

The considered monitoring sensor is the RedEdge-M crop sensor from Micasense ([www.micasense.com](http://www.micasense.com)). This multi-spectral camera captures simultaneously five discrete bands (BLUE, GREEN, RED, REDEGE and NIR) and uses narrowband filters to obtain accurate measurements of reflectance. Furthermore, a downwelling light sensor is connected to the camera to improve the radiometric quality of the dataset. A GPS is also employed to geo-referencing the multispectral images acquired during the survey. The RedEdge-M performance varies with the UAV altitude. In particular, the grid spacing requirement must be defined according to the flight altitude as reported in Fig. 2.

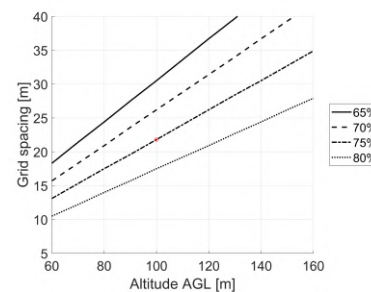


Fig. 2: RedEdge-M grid spacing requirement with respect to UAV altitude.

### B. Olcenengo Paddy Field Scenario

The first scenario envisions a paddy field (see Fig. 3(a)) at Olcenengo, Vercelli, Italy ( $45^{\circ}22'22.2''N$ ,  $8^{\circ}17'34.3''E$ ). A

grid pattern allows to provide the required field coverage in compliance with the performance index of interest and the payload characteristics, i.e. a RedEdge-M multi-spectral camera.



Fig. 3: (a) Olcenengo paddy field aerial view (credit: Google) and (b) grid pattern with 27 waypoints.

Therefore, the grid width has been set in compliance with sidelap and overlap required by the *passive* sensor itself, and including also an external band to allow the FW-UAV stabilization after each turn. The UAV flight mission is represented by a grid pattern, identified by 27 waypoints and represented in Fig. 3(b), over a  $200 \times 150$  m rectangular-shape area. The grid-width is given by the sensor performance with respect to the flight altitude (see Section II-A for further details) and has been set to 20 m considering an altitude of 100 m, including a 75% of both overlap and sidelap requirements, following the sensor manufacture guidelines described in [16]. Moreover, the reference airspeed  $u_{ref}$  has been set to 13.5 m and the coverage area includes also a 10 m band to allow the UAV stabilization after each turn.

### C. Carpeneto Vineyard Scenario

The second scenario proposed involves a Dolcetto vineyard at Carpeneto, Alessandria, Italy ( $44^\circ 40' 55.6''N$ ,  $8^\circ 37' 28.1''E$ ). In this case, the Mission Planner of ArduPilot open source autopilot has been used to identify a grid pattern over the vineyard of interest, represented in Fig. 4(a). The main difference with respect to the paddy field scenario is represented by a sloped terrain, which requires an additional control for the altitude to guarantee required terrain following task.

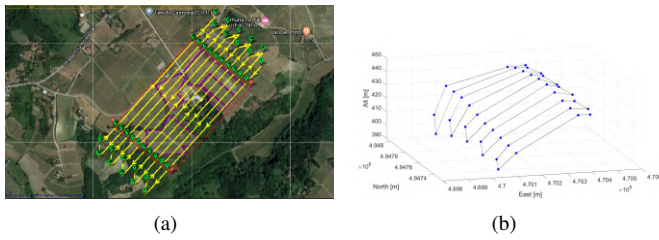


Fig. 4: Top view of the waypoints distribution over the vineyard (a) and related 3D trajectory (b).

The grid is characterized by a peculiar path orientation with respect to the grapevine rows, as highlighted in Fig. 4(a) and in particular, this scenario requires the UAV to maintain a 150 m relative altitude (see Fig. 4(b)) with respect to the terrain, envisioning a constant airspeed profile with  $u_{ref} = 12$  m/s.

## III. SIMULATION ENVIRONMENT

The development of a system containing embedded software involves many test activities at different stages in the development process. First, a reliable simulation environment shall be developed, verified and validated via Software in the Loop (SIL) simulations, in which the embedded software is tested within a simulated environment model.

Consequently, a SIL multi-rate simulator has been realized in a MATLAB/Simulink environment to perform preliminary validation of the flight software running over an Intel Core i7 – 7500U with a CPU @2.70 GHz, a RAM of 16 GB and a 512 GB solid-state drive. Fixed-step integration with an *ode4* solver and a sample frequency of 100 Hz is performed.<sup>1</sup> The FW-UAV nonlinear dynamics model implemented in this work can be found in [17] while a thorough overview of the waypoint-based guidance algorithm and the longitudinal and lateral-directional TRMPC schemes are provided in Section III-A and Section III-B, respectively. Further details can be found in [18].

### A. Waypoint-based Guidance Algorithm

The waypoint-based guidance algorithm proposed in [19] has been selected for this work due to its low complexity and high reliability as already demonstrated in [7]. The guidance algorithm has a fixed sample frequency of 10 Hz. As presented in [19] the guidance profile is mainly split into three phases and a given set of waypoints  $WP_i$  is considered, defined in terms of North and East coordinates, i.e.  $N_i$  and  $E_i$ , respectively. In [19], the altitude of each waypoint was considered fixed and constant during flights. Instead, in this work real flight data, collected during previous flight tests, have been used as reference altitude values to feed the MPC terrain following algorithm presented in Section III-B. In particular, let us consider two consecutive WPs, i.e.  $WP_j$  and  $WP_{j+1}$ , defined by  $N_j, E_j, H_j$  and  $N_{j+1}, E_{j+1}, H_{j+1}$  North-East-Down coordinates, respectively. The terrain following guidance is based on a *ramp* function that allows to follow the terrain profile accordingly defining the time-varying reference altitude signal  $h_{ref}(t)$  fed to the control scheme as

$$h_{ref}(t) = \frac{H_{j+1} - H_j}{\sqrt{(N_{j+1} - N_j)^2 + (E_{j+1} - E_j)^2}} \cdot d(t) + H_j, \quad (1)$$

where  $d(t)$  is the time-varying relative distance among the aircraft, with North-East coordinates given as  $(N_{UAV}(t), E_{UAV}(t))$ , and the  $j$ -th WP and  $d(t)$  is defined by

$$d(t) = \sqrt{(N_{UAV}(t) - N_j)^2 + (E_{UAV}(t) - E_j)^2}. \quad (2)$$

<sup>1</sup>It is important to highlight that, while the system dynamics and the guidance algorithm work at 100 Hz, the control algorithm is updated with a 10 Hz frequency. Thus, the system is fed with the same constant control output for ten consecutive steps, until the control algorithms is run again, initialized with new initial conditions.

## B. Tracking Tube-based Robust MPC

Consider the following discrete time-invariant state-space system in which persistent disturbances  $w_k$  are included

$$x_{k+1} = A_d x_k + B_d u_k + w_k, \quad (3)$$

where  $x_k$  and  $u_k$  represent the discrete-time state vector and the control signal at time  $k$ , respectively. In particular, the state variables in the longitudinal plane are the longitudinal component of the total airspeed in body axes  $u$ , the angle of attack  $\alpha$ , the pitch angle  $\theta$ , the pitch rate  $q$ , and the altitude  $h$  whereas for the lateral-directional plane the state vector includes the  $\beta$ , the roll rate  $p$ , the yaw rate  $r$  and the roll angle  $\phi$ . To achieve tracking, at steady state we shall have  $x_{k+1} = x_k = r_k$ . Hence, the system dynamics (3) can be rewritten in terms of the state deviation  $\delta x_k$  with respect to the reference  $r_k$ , i.e.  $\delta x_k = x_k - r_k$ , as follows

$$\delta x_{k+1} = A_d \delta x_k + B_d u_k + w_k. \quad (4)$$

Let's assume that the system is required to satisfy hard constraints on both state and input, i.e.  $x_k \in \mathbb{X}$  and  $u_k \in \mathbb{U}$ , where  $\mathbb{X} \subset \mathbb{R}^n$  and  $\mathbb{U} \subset \mathbb{R}^m$  are compact and convex polytopes whereas the disturbance  $w_k$  is an independent and identically distributed (i.i.d.) zero-mean random variable, with a convex and bounded support  $\mathbb{W} \subset \mathbb{R}^n$ , all containing the origin. The TRMPC approach is based on the concept of *tube* of state trajectories, each one representing an admissible disturbance sequence over the observed time-window. The center of this tube corresponds to the nominal undisturbed trajectory, which dynamics is defined as

$$\delta z_{k+1} = A_d \delta z_k + B_d v_k, \quad (5)$$

where  $z_k$  and  $v_k$  are the discrete-time undisturbed, nominal state and input, respectively. Then, a time-varying feedback control law of the form

$$u_k = v_k + K(\delta x_k - \delta z_k), \quad (6)$$

has been exploited for the optimization problem, where the feedback gain matrix  $K$  is defined such that the closed-loop dynamics, i.e.  $A_K = A_d + B_d K$ , is quadratically stable. The appealing aspect of this robust control algorithm is intrinsic in the evaluation of the gain matrix. Indeed,  $K$  can be evaluated *offline* to significantly reduce the *online* computational cost. Further details can be found in [10] and [12].

As previously anticipated, two different tracking-TRMPC schemes have been implemented to control the FW-UAV linearized error dynamics with respect to the time-varying reference signals generated by the guidance algorithm, i.e. the airspeed  $u_{ref}$ , the altitude  $h_{ref}(t)$ , and the roll angle  $\phi_{ref}(t)$ .<sup>2</sup> Hence, the longitudinal TRMPC receives in input the reference velocity and altitude and provides as control output the throttle command  $\Delta T$  and the elevator deflection  $\delta_e$ , the former acting on the velocity  $u$  and the latter on the pitch

<sup>2</sup>A dedicated PID scheme is in charge of controlling the heading angle  $\psi$  to follow the relative reference signal  $\psi_{ref}(t)$  and provides as main output the reference roll angle  $\phi_{ref}(t)$

angle  $\theta$ . On the other hand, the lateral-directional TRMPC receives the reference heading angle  $\phi_{ref}(t)$  to supply the system with the optimal aileron deflection  $\delta_a$ , which acts on the bank angle  $\phi$ , at each time step  $k$ . Consequently, according to the tracking constraints inherited from the specific mission scenario, the state and control input constraints have been set envisioning the presence of a fixed-direction wind turbulence, modeled as random noise with uniform distribution and maximum intensity of  $\pm 1$  m/s, representing the bounded persistent disturbance affecting the FW-UAV dynamics.

The TRMPC here proposed allows to steer the uncertain trajectories to the nominal one, controlling the "center" of this tube via a classical MPC approach. In order to ensure the robustness of the algorithm, the constraint set imposed on the nominal system are tightened with respect to the initial ones as a function of the minimal Robust Positive Invariant set  $S_K(\infty)$  for the error dynamics

$$e_{k+1} = A_K e_k + w_k, \quad (7)$$

where  $S_K(\infty)$  is defined as

$$S_K(\infty) = \sum_{\ell=1}^{\infty} A_K^\ell \mathbb{W} \quad (8)$$

and can be evaluated following the guidelines provided in [10]. Thus, the tightened state and input constraint sets, i.e.  $\mathbb{Z}$  and  $\mathbb{V}$ , can be obtained as

$$\mathbb{Z} = \mathbb{X} \ominus S_K(\infty), \quad (9a)$$

$$\mathbb{V} = \mathbb{U} \ominus K S_K(\infty). \quad (9b)$$

## IV. SOFTWARE-IN-THE-LOOP RESULTS

Preliminary SIL testing results related to the Olcenengo paddy field and to the Carpeneto vineyard are here presented. For each scenario, two different SIL simulations have been performed, considering either the presence or the absence of a fixed-direction wind turbulence as disturbance source, exploiting the same setting parameters.

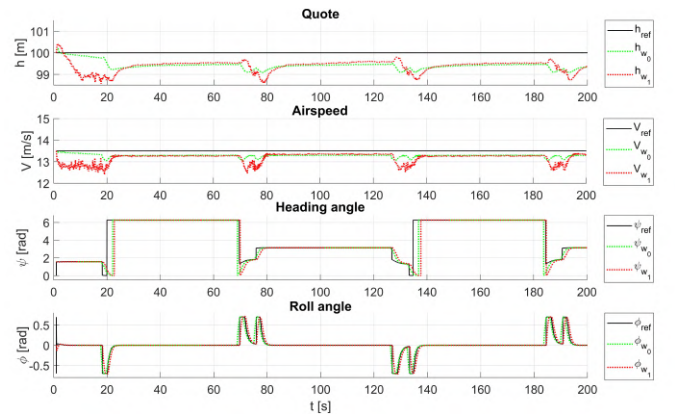


Fig. 5: Controlled state variables for the paddy field.

First, Fig. 5 and Fig. 6 show the TRMPC tracking capabilities for UAV translational and attitude control and terrain

following tasks.<sup>3</sup> The simulation results prove the robustness and the efficacy of the control strategy since all the constraints are fulfilled, even when the disturbance is active. Moreover, it appears evident that the UAV attitude is less affected by the wind turbulence, i.e. excellent tracking with or without wind turbulence. On the other hand, the effect of disturbance are more evident on UAV airspeed and altitude, in particular in the WP proximity and during turning phases.

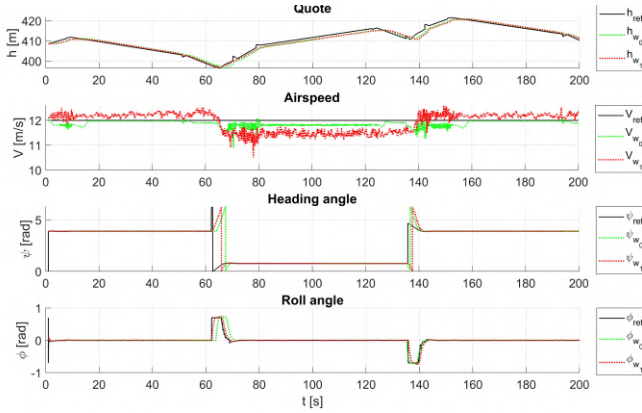


Fig. 6: Controlled state variables for the vineyard.

Fig. 7 and Fig. 8 represent the control input profile for the paddy field and the vineyard scenarios, respectively, comparing the control behavior when no disturbance is acting on the system (black line figures) with the case of wind turbulence affecting the UAV dynamics (red line figures).

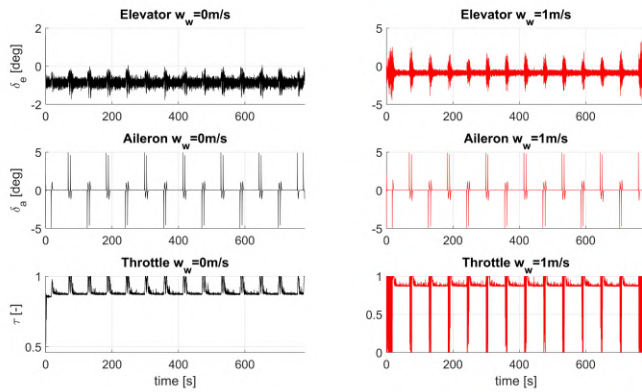


Fig. 7: Control input variables for the paddy field.

It is possible to observe in both scenarios the greater control effort required to the aircraft when the wind is envisioned. In particular, the throttle command  $\Delta T$  results the most affected by the disturbance source since it is acting on the aircraft airspeed  $u$ , which in turn is directly affected by the wind turbulence. On the other hand, elevator and aileron deflections present significant variations only in correspondence with the WPs turning phases. Moreover, we can observe in Fig. 8 that

<sup>3</sup>The results are shown only for the first 200 s of simulation to better highlight the control capabilities.

the longitudinal control commands result higher than those in Fig. 7 because of the non-constant altitude profile.

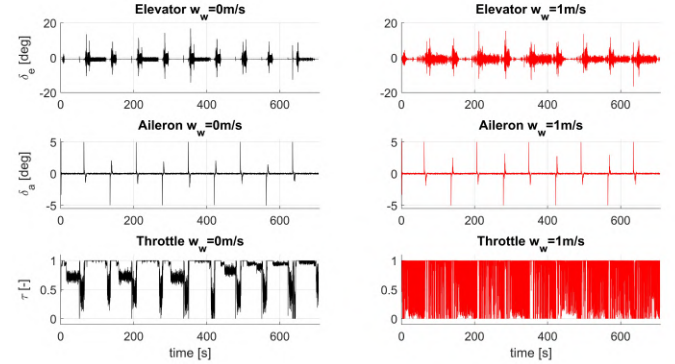


Fig. 8: Control input variables for the vineyard.

Last, Fig. 9 and Fig. 10 represent the final trajectories over the paddy field and the vineyard, respectively, in which it is possible to retrace the same behaviors previously described. In particular, the more significant impact of the wind turbulence can be observed on the vertical component of the motion whereas the effective lateral-directional control allows an almost perfect alignment of the undisturbed/disturbed trajectories in the North-East plane, as highlighted in Fig. 9(b) and Fig. 10(b).

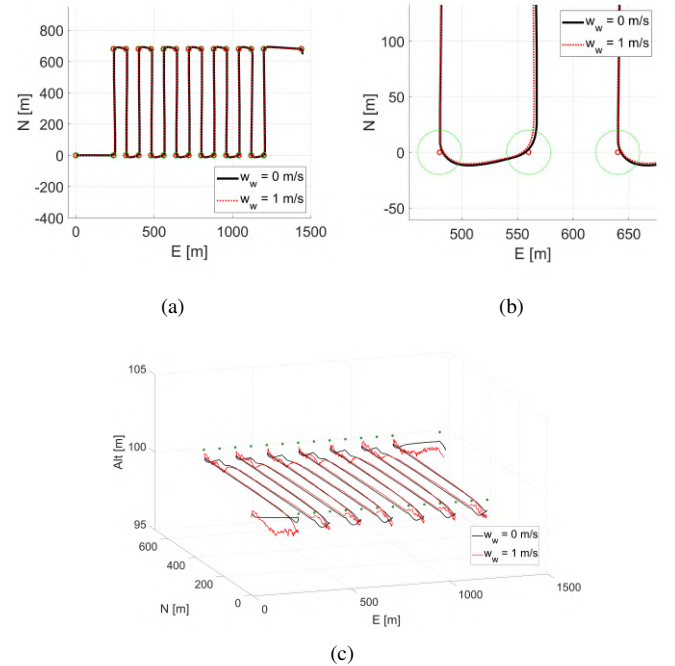


Fig. 9: Paddy field trajectories on the North-East plane with and without wind turbulence (a); zoom-in on the 2D trajectories (b); and 3D trajectories (c).

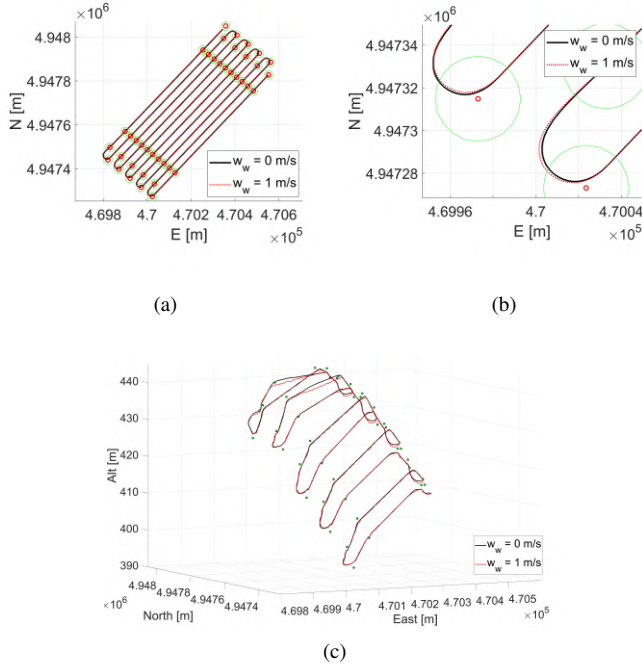


Fig. 10: Vineyard trajectories on the North-East plane with and without wind turbulence (a); zoom-in on the 2D trajectories (b); and 3D trajectories (c).

## V. CONCLUSIONS AND FUTURE WORKS

A combination of waypoint-based guidance algorithm and a tracking TRMPC control is proposed for Fixed-Wing Unmanned Aerial Vehicles (FW-UAVs) in the presence of wind disturbance to perform remote sensing and terrain following tasks over different crop fields. In particular, the effectiveness of the strategy proposed has been preliminary shown via simulations for a paddy field, i.e. constant altitude, and a vineyard, envisioning a terrain following approach. The results obtained shows the TRMPC capability of matching good stability performance of the platform and remarkable tracking capabilities.

## REFERENCES

- [1] D. Rose and J. Chilvers, "Agriculture 4.0: responsible innovation in an era of smart farming," *Frontiers in Sustainable Food Systems*, vol. 2, p. 87, 2018.
- [2] G. Sylvester, "E-agriculture in action: Drones for agriculture," *Published by Food and Agriculture Organization of the United Nations and International Telecommunication Union, Bangkok*, 2018.
- [3] F. M. Jiménez-Brenes, F. López-Granados, J. Torres-Sánchez, J. M. Peña, P. Ramírez, I. L. Castillejo-González, and A. I. de Castro, "Automatic uav-based detection of cynodon dactylon for site-specific vineyard management," *PloS one*, vol. 14, no. 6, p. e0218132, 2019.
- [4] L. Comba, P. Gay, J. Primicerio, and D. R. Aimonino, "Vineyard detection from unmanned aerial systems images," *computers and Electronics in Agriculture*, vol. 114, pp. 78–87, 2015.
- [5] A. Khaliq, L. Comba, A. Biglia, D. Ricauda Aimonino, M. Chiaberge, and P. Gay, "Comparison of satellite and uav-based multispectral imagery for vineyard variability assessment," *Remote Sensing*, vol. 11, no. 4, p. 436, 2019.

- [6] J. Albetis, A. Jacquin, M. Goulard, H. Poilvé, J. Rousseau, H. Clenet, G. Dedieu, and S. Duthoit, "On the potentiality of uav multispectral imagery to detect flavescence dorée and grapevine trunk diseases," *Remote Sensing*, vol. 11, no. 1, p. 23, 2019.
- [7] M. Mammarella, E. Capello, F. Dabbene, and G. Guglieri, "Sample-based smpc for tracking control of fixed-wing uav," *IEEE control systems letters*, vol. 2, no. 4, pp. 611–616, 2018.
- [8] K. Alexis, C. Papachristos, R. Siegwart, and A. Tzes, "Robust model predictive flight control of unmanned rotorcrafts," *Journal of Intelligent & Robotic Systems*, vol. 81, no. 3, pp. 443–469, 2016.
- [9] N. Michel, S. Bertrand, G. Valmorbidia, S. Oлару, and D. Dumur, "Design and parameter tuning of a robust model predictive controller for uavs," in *20th IFAC World Congress*, 2017.
- [10] D. Mayne and J. Rawlings, *Model Predictive Control: Theory and Design*. Nob Hill Publishing, 2009.
- [11] B. Sakhdari, E. M. Shahrivar, and N. L. Azad, "Robust tube-based mpc for automotive adaptive cruise control design," in *2017 IEEE 20th International Conference on Intelligent Transportation Systems (ITSC)*. IEEE, 2017, pp. 1–6.
- [12] M. Mammarella, E. Capello, H. Park, G. Guglieri, and M. Romano, "Tube-based robust model predictive control for spacecraft proximity operations in the presence of persistent disturbance," *Aerospace Science and Technology*, 2018.
- [13] S. Petkar, S. Umbarkar, M. Mejari, N. Singh, and F. Kazi, "Robust tube based mpc for pvtol trajectory tracking using systems flatness property," in *2016 International Conference on Unmanned Aircraft Systems (ICUAS)*. IEEE, 2016, pp. 1095–1101.
- [14] E. Capello, D. Sartori, G. Guglieri, and F. Quagliotti, "Robust assessment for the design of multi-loop proportional integrative derivative autopilot," *IET Control Theory Applications*, vol. 6, no. 11, pp. 1610–1619, 2012.
- [15] T. Erkkinen and M. Conrad, "Verification, validation, and test with model-based design," SAE Technical Paper, Tech. Rep., 2008.
- [16] L. N. Mascarello, F. Quagliotti, and G. Ristorto, "A feasibility study of an harmless tiltrotor for smart farming applications," in *Unmanned Aircraft Systems (ICUAS), 2017 International Conference on*. IEEE, 2017, pp. 1631–1639.
- [17] B. Etkin and L. Reid, *Dynamics of Flight: Stability and Control*. New York: John Wiley and Sons, 1996.
- [18] M. Mammarella and E. Capello, "Tube-based robust mpc processor-in-the-loop validation for fixed-wing uavs," *Journal of Intelligent and Robotic Systems (under review)*.
- [19] E. Capello, G. Guglieri, and G. Ristorto, "Guidance and control algorithms for mini-UAV autopilots," *Aircraft Engineering and Aerospace Technology*, vol. 89, no. 1, pp. 133–144, 2017.
- [20] H. Chao, Y. Cao, and Y. Chen, "Autopilots for small unmanned aerial vehicles: A survey," *International Journal of Control, Automation and Systems*, vol. 8, no. 1, pp. 36–44, 2010.
- [21] R. García, F. Rubio, and M. Ortega, "Robust pid control of the quadrotor helicopter," *IFAC Proceedings Volumes*, vol. 45, no. 3, pp. 229 – 234, 2012.
- [22] J. Dávila and S. Salazar, "Robust control of an uncertain uav via high-order sliding mode compensation," *IFAC-PapersOnLine*, vol. 50, no. 1, pp. 11 553–11 558, 2017.
- [23] J. Lesprier, J.-M. Biannic, and C. Roos, "Modeling and robust nonlinear control of a fixed-wing uav," in *2015 IEEE Conference on Control Applications (CCA)*. IEEE, 2015, pp. 1334–1339.
- [24] A. Brezoescu, T. Espinoza, P. Castillo, and R. Lozano, "Adaptive trajectory following for a fixed-wing uav in presence of crosswind," *Journal of Intelligent & Robotic Systems*, vol. 69, no. 1-4, pp. 257–271, 2013.
- [25] E. Capello, G. Guglieri, P. Marguerettaz, and F. Quagliotti, "Preliminary assessment of flying and handling qualities for mini-uavs," *Journal of Intelligent & Robotic Systems*, vol. 65, no. 1, pp. 43–61, 2012.
- [26] F. Gavilan, R. Vazquez, and S. Esteban, "Trajectory tracking for fixed-wing uav using model predictive control and adaptive backstepping," *IFAC-PapersOnLine*, vol. 48, no. 9, pp. 132–137, 2015.
- [27] M. Kamel, T. Stastny, K. Alexis, and R. Siegwart, *Model Predictive Control for Trajectory Tracking of Unmanned Aerial Vehicles Using Robot Operating System*. Springer International Publishing, 2017, pp. 3–39.
- [28] T. J. Stastny, A. Dash, and R. Siegwart, "Nonlinear mpc for fixed-wing uav trajectory tracking: Implementation and flight experiments," in *AIAA Guidance, Navigation, and Control Conference*, 2017, p. 1512.